

Recovery of edge moments of the current density profile in a tokamak from external magnetic measurements

P.J. Mc Carthy¹, ASDEX Upgrade Team²

¹*Physics Dept, University College Cork, Association EURATOM-DCU, Cork, Ireland*

²*Max-Planck-Institut für Plasmaphysik, Euratom Association, Garching, Germany*

Introduction

The reconstruction of ideal MHD equilibrium states from external magnetic measurements plays a central role in the operation of tokamak experiments. The realtime availability of equilibrium parameters, both by non-iterative methods such as Function Parameterization [1] and realtime versions of interpretive codes such as EFIT [2] provides essential input for modern feedback control algorithms which are continuously growing in complexity [3]. It has been a standard assumption [4] that information on the internal current density and pressure profiles provided by magnetics is limited to three integral moments, namely the plasma current $I_p = \int_A j_\phi dA$, beta poloidal $\beta_p = 2\mu_0 \int_V p dV / (V \bar{B}_{\theta_b}^2)$ and internal inductance $l_i = \int_V B_\theta^2 dV / (V \bar{B}_{\theta_b}^2)$ where j_ϕ is the toroidal current density, $\bar{B}_{\theta_b} = \mu_0 I_p / \int_b d\ell$ is the average value of the poloidal magnetic field on the boundary b , and V and A denote the plasma volume and cross-sectional area. Here we present an analytical example and experimental results showing that additional moments of j_ϕ , strongly localized in the edge region of the plasma, are recoverable from magnetics when the plasma is bounded by a separatrix with one or more X-points.

Theory

The identifiability of edge moments of the j_ϕ profile can be demonstrated from the following simple analytic model: The flux function per unit length for two parallel wires along the z direction which pass through $x = 0$, $y = \pm d$ and carry equal current I is

$$\Psi(x, y) = \frac{\mu_0 I}{2\pi} \ln \frac{d^2}{\sqrt{x^2 + (y-d)^2} \sqrt{x^2 + (y+d)^2}} \quad (1)$$

The doublet shape has a single X-point at the origin and the upper separatrix contour is bounded by $-d/2 \leq x \leq d/2$ and $0 \leq y \leq \sqrt{2}d$. Calculation of the cross-sectional area $A(\rho)$ yields

$$A(\rho) = d^2 \sqrt{1 - \rho^2} \left(E \left[(1 - \rho^{-2})^{-1} \right] - K \left[(1 - \rho^{-2})^{-1} \right] \right) \quad (2)$$

where the normalized horizontal radius ρ satisfies $\rho = e^{-\psi}$ with $\psi = 2\pi\Psi/\mu_0 I$, K and E are complete elliptic integrals of the first and second kind, and $\lim_{\rho \rightarrow 1} A(\rho) = d^2$. Calculation of the flux surface average of the y coordinate as a function of ρ yields

$$\langle y \rangle_\rho = \oint \frac{y d\ell}{|\nabla \psi|} / \oint \frac{d\ell}{|\nabla \psi|} = \frac{\pi d \sqrt{1 - \rho^2}}{2K[(1 - \rho^{-2})^{-1}]} \quad (3)$$

As $\rho \rightarrow 1$, eq. 3 scales as $\langle y \rangle_\rho \sim -1/\ln(1-\rho)$ and so $\langle y \rangle$ falls to zero at $\rho = 1$ due to the progressive localization around the X-point of the area in the annular interval $\{\rho, 1\}$. This localization extends further into the plasma when $\langle y \rangle$ is expressed in terms of the radial parameter v defined as the normalized distance to the point of intersection with the flux surface along the line joining the magnetic axis to the X-point (see fig. 1(a)). For the wire model, $v = 1 - \sqrt{1 - \rho}$.

The qualitative features in the above analysis apply to X-point tokamak equilibria whose flux surfaces possess the same essential topological features. In particular, the localization of annular areas above the X-point allows the identification of edge moments of j_ϕ since the current flowing in this region is comparable to a local distribution near the X-point, distinct from the main current distribution and therefore readily identifiable by magnetics. For quantitative results

we consider an ASDEX Upgrade single null equilibrium (figure 1) with tangential and normal magnetic probes located on an idealized contour conformal to the separatrix but scaled up by 40%, a factor typical for probe-separatrix distances. Flux surface integrals of the Greens function versus v at each of P probe sites were carried out numerically to generate $2P$ radial influence profiles. For simplicity, the flux surface averaged current density $\langle j_\phi \rangle$ was used to calculate the Greens function integrals.

Sample profiles plotted in figure 1(b) all have the property that they are nearly independent of v in the plasma core, but change, very dramatically in the case of probes near the X-point, as $v \rightarrow 1$. It is this strong variation towards the plasma boundary that enables identification of edge moments of $\langle j_\phi \rangle$. The influence profiles were discretized into $N = 400$ radial elements to form an $N \times 2P = 400 \times 120$ influence matrix \mathcal{G} where the influence profile of each annulus was scaled by its annular current and a total of 1 MA was distributed over the plasma cross-section. A Singular Value Decomposition (SVD) of \mathcal{G} resulted in the ordered sequence of singular values (in mT) $\{\sigma_i\} = \{1902, 226, 61.4, 18.9, 6.1, 1.9, \dots\}$. These magnitudes, which describe the typical amplitude associated with the corresponding singular vectors (SVs), give a practical measure of the recoverability of moments of the current profile described by the SVs when compared to experimentally known measurement uncertainties in the magnetic signals.

For the idealized probe geometry used here, $\sigma_1 - \sigma_4$ are well above the median fit error of 1.3 mT for equilibrium reconstructions on ASDEX Upgrade using the CLISTE code [5] and hence correspond to 4 clearly identifiable moments of $\langle j_\phi \rangle$. The leading two moments correspond to the plasma current and internal inductance l_i and all subsequent moments are localized towards the edge. The singular values satisfy $\sum_i \sigma_i^2 = \sum_{j=1}^P (B_{j,\parallel}^2 + B_{j,\perp}^2)$ where $B_{j,\parallel}$ and $B_{j,\perp}$ are the components of the poloidal magnetic field at the j th probe site due to a 1 MA plasma current. If L_S and L_P denote the circumferences of the separatrix and probe contours, respectively, then for plasma current I_p and P probe sites, the singular values scale as $\sigma_j \sim \sqrt{P} I_p (L_S/L_P)^j$.

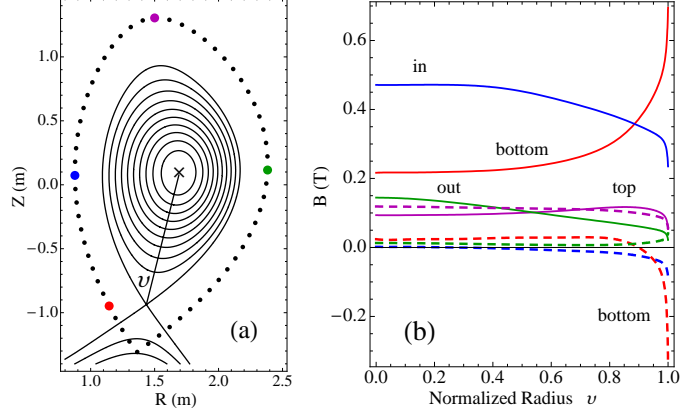


Figure 1: (a) Lower null ASDEX Upgrade equilibrium with $P = 60$ equidistant magnetic probe sites on an idealized measurement contour conformal with the separatrix and scaled up by 40%. (b) tangential (—) and normal (---) components of the poloidal magnetic field per MA annular current for the four sites highlighted in figure 1(a) versus the flux label v .

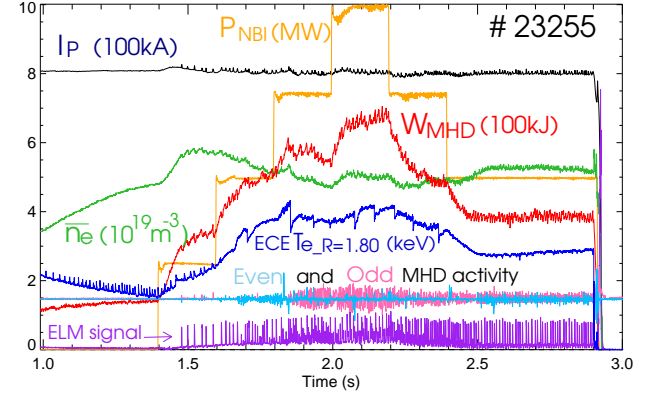


Figure 2: Time traces of plasma current I_p , line-integrated density \bar{n}_e , neutral beam injection heating power P_{NBI} , plasma stored energy W_{MHD} , electron temperature T_e at major radius $R = 1.8$ m, MHD even and odd mode signals, and divertor tile currents (ELM signal) for ASDEX Upgrade discharge # 23255. The CLISTE analysis is for the time window $1.2 \leq t \leq 2.7$ s.

The foregoing analysis is incomplete in several respects: A fixed flux surface topology is used and hence the known dependence of magnetics on the Shafranov shift is not reflected in the SVs. Also, the use of $\langle j_\phi \rangle$ conceals the major radius dependence of the j_ϕ profile. Current flow in the scrape-off layer (SOL) outside the separatrix is not considered. These aspects are all taken into account in the CLISTE interpretive equilibrium code [5,6] which generates MHD equilibrium solutions on ASDEX Upgrade constrained by data from multiple diagnostics. Source profiles extend into the SOL, where they can be constrained using pressure data and shunt resistance measurements of poloidal currents flowing in the axisymmetric divertor. The SVD analysis demonstrates that magnetics contain information on the edge current distribution, however use of the present SVD approach under realistic conditions for solving the equilibrium problem proved impractical and instead, for modelling flexibility, a cubic spline model with, typically, 9 radial knots is used to parameterize the $p'(\psi)$ and $ff'(\psi)$ source profile shapes. This amounts to 18 free shape parameters, well in excess of the number of identifiable moments of the current distribution. Regularization of the magnitude of the fitted spline coefficients and/or the curvature at each knot position controls the ill-conditioned nature of the problem.

Experimental Results

The recoverability of edge moments of the current density profile is illustrated by a sequence of CLISTE equilibria for ASDEX Upgrade discharge 23255, $I_p = 800$ kA, $B_t = -2.5$ T, $\bar{n}_e = 5.8 \times 10^{19} \text{ m}^{-3}$ which had a stationary low power phase consisting of 0.3 MW ohmic heating and 0.5 MW ECRH, followed by the addition of four 2.5 MW neutral beams at 200 ms intervals (fig. 2) which yielded a factor of six variation in the stored energy during the current flattop phase.

A spline model with 9 internal knots for the $p'(\psi)$ and $ff'(\psi)$ source profiles regularized by penalizing both the curvature at each knot location and also the magnitude of the fitted coefficients was used to find free boundary equilibria constrained by 60 magnetic signals at 10 ms intervals for the time window $1.2 \leq t \leq 2.7$ s, with ELM timepoints excluded. Since sawteeth were present throughout most of the time window, the safety factor q on the magnetic axis was clamped at a value just below unity. The rms (root mean square) fit error was 1.0 mT or 0.9% of the rms signal magnitude. The same spline model, with identical regularization penalties, was also used to generate equilibria additionally constrained by pressure data in the range $0.85 \leq \rho_{pol} \leq 1.02$ obtained from high resolution n_e , T_e and T_i data from the Lithium beam

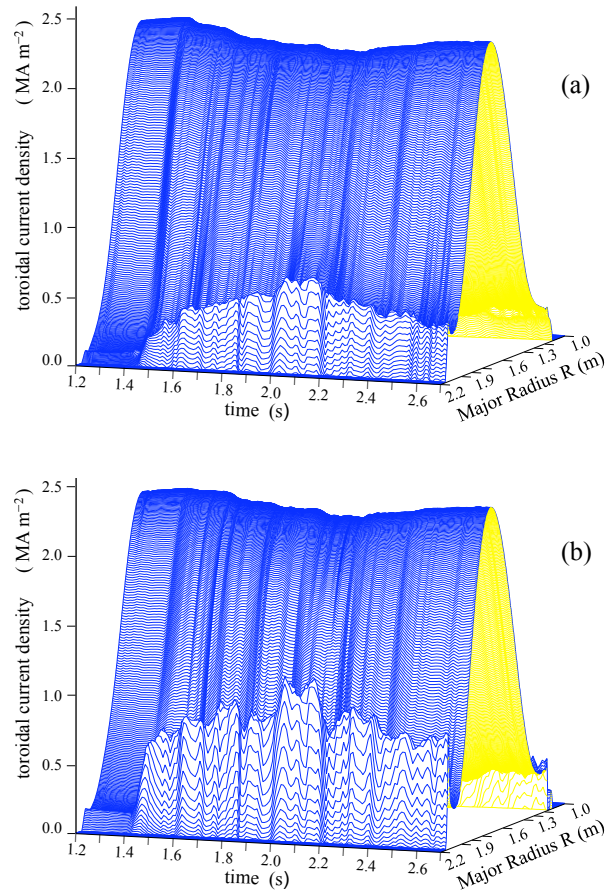


Figure 3: Time evolution of the j_ϕ profile as a function of major radius along the magnetic midplane as reconstructed by CLISTE from (a) magnetic data and (b) a combination of magnetic and edge pressure data.

[7,8] , ECE [9] and Thomson scattering [10] diagnostics. The magnetic fit error was unchanged, and the rms pressure fit error was ≈ 150 Pa or 2.5% of the rms value of ≈ 6 kPa for $\rho_{pol} \geq 0.85$. Figure 3 shows the time evolution of the j_ϕ profile as a function of major radius along the magnetic midplane from CLISTE reconstructions using (a) magnetic data and (b) a combination of magnetic and edge pressure data.

In each case, a prominent edge peak in j_ϕ develops following the start of NBI heating at $t = 1.4$ s. It increases with heating power, reaching a maximum at $t = 2.2$ s just as the NBI power is reduced from its peak value. The evolution of the edge peak is very similar in both cases, although the inclusion of the pressure constraints results in the peak height in figure 3(b) exceeding that in 3(a) by a factor of ≈ 2 . Quantitative agreement between both fits is achieved when the toroidal current ' I_{edge} ' flowing outside a fixed flux surface close to the peak position is calculated in both cases. Figure 4 shows that the current flowing outside the $v = 0.9$ flux surface in both cases is nearly identical and scales closely with β_{pol} , consistent with a bootstrap-dominated current drive in the pedestal.

Conclusions

The analytical examples combined with the qualitative consistency between figure 3(a) and 3(b) and the quantitative agreement between the I_{edge} time traces in figure 4 allow the following conclusions to be drawn: Equilibrium magnetic measurements yield information on the j_ϕ profile near the boundary of an X-point plasma. Quantitative details of the profile shape cannot be identified from magnetics alone, but the current flowing outside a reference flux surface near the separatrix, in the vicinity of $v = 0.9$ is robustly determined. The fact that this region coincides with that of high pressure gradients and therefore high current densities associated with the edge transport barrier characteristic of the H-mode offers vital additional diagnostic information in the challenge to accurately determine the stability limits affecting ELM dynamics and to investigate wider issues of pedestal physics.

REFERENCES

- [1] P.J. Mc Carthy and F.C. Morabito, Int. J. Appl. Electromag. Mech. **8** 343 (1997).
- [2] L. L. Lao *et al.*, Fusion Sci. Tech. **48** 968 (2005).
- [3] W. Treutterer *et al.* Fusion Eng. Design **84** 1871 (2009).
- [4] L. L. Lao *et al.*, Nucl. Fusion **25** 1611 (1985).
- [5] P.J. Mc Carthy, Phys. Plas. **5** 3054 (1999).
- [6] W. Schneider *et al.*, Fusion Eng. Des. **48** 127 (2000).
- [7] M Reich, E. Wolfrum *et al.*, Plas. Phys. Control. Fusion **46** 797 (2004).
- [8] E. Wolfrum, J. Schweinzer *et al.*, Rev. Sc. Inst. **77** 003507 (2006).
- [9] N.K. Hicks, W. Suttrop *et al.*, Fusion Sci. Tech. **57** 1 (2010).
- [10] B. Kurzan, H. Murmann, H. Salzmann, Rev. Sc. Inst. **72** 1111 (2001).

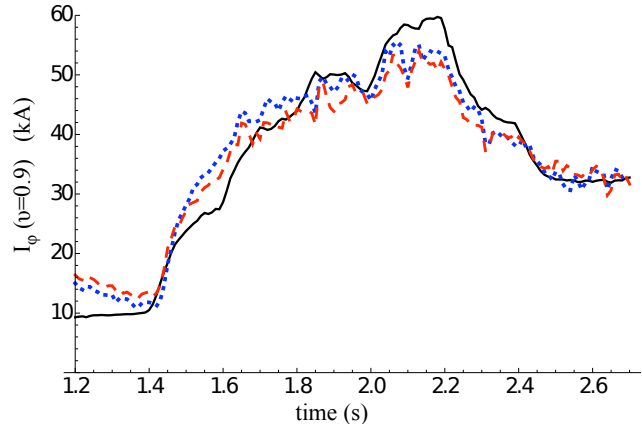


Figure 4: Time evolution of toroidal current outside the $v = 0.9$ surface (corresponding to $\rho_{pol} \approx 0.99$) for the magnetics-only fit (dots) and the magnetics + pressure fit (dashes). The solid curve is $\beta_{pol}(t)$ scaled by a factor of 37.0.